C. R. Physique 12 (2011) 180–185

Contents lists available at ScienceDirect

Comptes Rendus Physique

www.sciencedirect.com

Propagation and plasmas: new challenges, new applications

Modeling global ionosphere and inhomogeneities

Modélisation globale de l'ionosphère et inhomogénéités

Yannick Béniguel

IEEA, 13, promenade Paul-Doumer, 92400 Courbevoie, France

ARTICLE INFO

Article history:
Available online 3 March 2011

Keywords:
Plasma
Earth satellite navigation
Ionosphere

Mots-clés :
Plasma
Navigation par satellite
Ionosphère

ABSTRACT

A resolution of the plasma equations: continuity, momentum and energy applied to ionosphere modeling is presented. Two sub-models are described. The first one is a large scale model. It allows obtaining a medium's characterization over large distances both in altitude, including the essential part of the ionized medium, and in latitude around the magnetic equator. The second model is a local model aiming to characterize the bubble development and their behavior with respect to time. This characterization is required to assess propagation impairments for Earth satellite navigation, remote sensing and Earth satellite telecommunication as stated in a companion paper (Béniguel et al., 2011) [1].

RÉSUMÉ

Cet article présente une résolution des équations de plasma : équation de continuité et conservation de la quantité de mouvement et de l'énergie, appliquées à la modélisation de l'ionosphère. Deux modèles sont présentés : un modèle grande échelle permettant d'obtenir une caractérisation du milieu sur une plage d'altitude importante incluant l'essentiel du milieu ionisé et un large domaine de latitudes autour de l'équateur. Le second modèle est un modèle local permettant d'appréhender le développement d'inhomogénéités dans le milieu et leur évolution dans le temps. Cette connaissance est essentielle pour les problèmes liés à la navigation par satellite, l'observation de la terre et les télécommunications ainsi que présenté dans un article conjoint (Béniguel et al., 2011) [1].

1. Introduction

The ionosphere is the medium extending from approximately 60 km above the Earth's surface to about 2000 km. It is subject to permanent strong electron density variations with local time and location. The ionosphere state is linked to the solar activity, characterized by an 11 year cycle. A seasonal effect is superimposed to this cycle by the variation of the Earth's rotation axis with respect to the ecliptic. The ionosphere is, in addition, an anisotropic medium due to the influence of the Earth's magnetic field. It is usual to consider two states related to the mean values and to the fluctuations around these mean values. The mean values correspond to the "normal" or undisturbed ionosphere with no local or extended disturbances appearing. The disturbed state includes local or extended disturbances with perceptible variations to the ionosphere.

E-mail address: beniguel@ieea.fr.

1631-0705/$ – see front matter
doi:10.1016/j.crhy.2011.01.004

The models developed up to now, in general, consider the normal state. They can be placed into two categories: models based on physical analysis of ionosphere (the Chapman model is one reference) and models based on either statistical or theoretical evaluations used in propagation calculations. In the physical analysis of ionosphere, it is usually divided into three regions: D, E and F. The D region is between 60 and 90 km. The density of free electrons becomes practically zero at night. The E region extends from 90 km to 130 km. Its critical frequency is closely related to the incident solar radiation. The F region, situated above 130 km, has the strongest impact on satellite – Earth signals. The electron density reaches values greater than 10^{12} m^{-3}.

The ionosphere fluctuations are related to instability processes which develop inside the medium. Depletions of electron density, referenced as bubbles may appear mostly at low and high latitudes. The most important instability mechanisms contributing to the bubbles development are the gradient drift, the Rayleigh–Taylor and Kelvin–Helmholtz instabilities and the gravitational dependency. The way the bubbles develop depends on the altitude and they give rise to different characteristic dimensions [2]. In addition, the magnetic field plays an important role which results in elongated bubbles in that direction and consequently an anisotropic medium. The medium's drift velocity and its direction are also important parameters to be considered. Wave propagation through the ionosphere inhomogeneities leads to signal fluctuations referred as scintillations. Solving the navigation equations in this case adds positioning errors making this problem a major issue for satellite navigation systems (Béniguel et al.) [1].

Numerical models aiming to reproduce the electron density variations are presented in this article both for mean values and for the fluctuations. The approach uses the continuity, momentum and energy equations in both cases with simplified hypothesis. These two models, presented in Sections 2 and 3, differ in particular in the space step which is quite large in the first case in order to describe the whole medium. The second model uses a small space step and different assumptions in order to get some information on the bubbles development and their behavior with respect to the time.

2. First order model

A physical model proceeds from a resolution of the plasma equations inside the ionospheric region. Usually, only the plasma equations for ion O^+ are considered but as it implies chemical equilibrium relations, the other species, in particular N_2 and O_2 shall also be considered. It shall be noted that the thermosphere densities are given by O_2 and N_2 constituents. The first order ionosphere model that is presented here below, applies to the calculation of O^+ ion density. The electron density is assumed to be equal to this density, since the medium is electrically neutral. The other two constituents N_2 and O_2 are nevertheless considered in the calculation of electron–ion recombination.

The O^+ density is obtained by solving the medium's fluid equations, i.e. continuity, momentum and energy equations [3,4]. The continuity equation is given by:

$$\frac{\mathrm{d}N_\mathrm{i}}{\mathrm{d}t} = P_\mathrm{i} - L_\mathrm{i} - N_\mathrm{i}\nabla.v_\mathrm{d} - B\frac{\partial}{\partial s}\left(\frac{N_\mathrm{i}v_\mathrm{i}}{B}\right) \tag{1}$$

where P_i and L_i are the production and loss rates for O^+; v_d is the drift velocity; v_i is the ion velocity, s is the space coordinate and B is the Earth's magnetic field. The momentum equation may be written as:

$$v_\mathrm{i} - v_\mathrm{n} = -\frac{1}{m_\mathrm{i}\upsilon_\mathrm{in}}\left[\frac{kT_\mathrm{i}}{N_\mathrm{i}}\nabla N_\mathrm{i} + \frac{kT_\mathrm{e}}{N_\mathrm{e}}\nabla N_\mathrm{e} + k\nabla(T_\mathrm{i} + T_\mathrm{i}) - m_\mathrm{i}g\right] \tag{2}$$

where T_i and T_e are the electron and ion temperatures and v_n is the neutral wind velocity and υ_in is the collision frequency between the ions and the neutral particles. Solving these two equations results in a parabolic equation with respect to time.

2.1. Algorithm

The system of coordinates is the Mc Ilwain system [5] on which the system of equations can be written in a simplest way. The reduced normalized coordinates are named p and q. On a p line the longitude is fixed and it extends from negative latitude to positive latitude. The altitude increases along a p line with a maximum altitude at the equator. A succession of meridian planes with p lines is considered. This automatically defines the calculation domain. The p values that were defined in our calculation extend from 1 to 1.5. The maximum corresponding altitude is 1911 km. The difference in longitude of the meridian planes is small as compared to the time scale. It was set to 2° (480 s of Earth rotation) for the results hereafter presented. The reference axes in each meridian plane include the Earth's radius at the equator and the Earth's magnetic field. The meshing in the meridian plane forms symmetrical curves with respect to the equator. The corresponding altitude of each point along these curves presents its maximum at the equator and decreases with latitude. Consequently, the computation can be decreased with the latitudinal range as the altitude range is limited.

The model inputs include the densities of O, N_2 and O_2, the neutral temperatures, the production and loss rate of electrons, the neutral velocity and the vertical drift velocity.

These data may be selected from average profiles. This could be improved using measurement data. Temperature profiles for ions and electrons can be calculated solving the energy equation. However, the calculation is made easier using typical temperature profiles which allow skipping the energy equation.

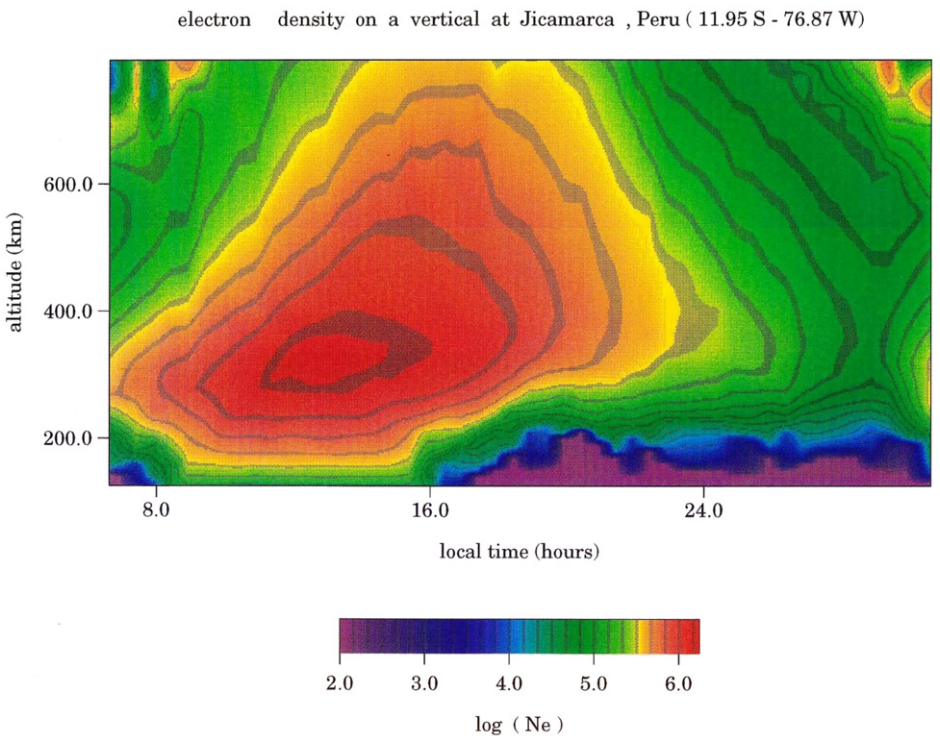

Fig. 1. Low latitude electron density versus altitude and local time. The maximum of ionization occurs at around 300 km. The electron content above the peak contributes significantly to the TEC value.

The parabolic equation obtained is solved by a Crank Nicholson fully implicit scheme. At the bottom of the mesh, the medium is assumed to be in photochemical equilibrium. An example of result is presented on Fig. 1. The ionization peak, Log (Ne) in electrons per cm^3, occurs at around 300 km at 12:00 to 14:00 local time. The electron content at higher altitudes is significant up to altitudes equal to more than 800 km.

The electron density profile obtained with the model developed (referenced IDEQ for Ionospheric Density at EQuatorial regions) has been compared with those provided by IRI90 (International Reference Ionosphere) [6] and PIM (Parameterized ionospheric Model) [7]. IRI90 is based on measurements. On the contrary PIM is a set of several sub-models with less stringent hypothesis and which should give more accurate results. The vertical space step was set to 10 km in this example.

Fig. 2 shows a comparison between the three models. Below the peak the PIM result and the one that was obtained with the model presented in this paper compare quite well. Above the peak, discrepancies arise. This may be due to simplified hypothesis in the input data set that was considered, in particular due to the fact that some of parameters, as the drift velocity for instance, did not vary with altitude. Higher order models should increase the accuracy and would probably give a better agreement at high altitudes.

3. Second order model

The second order model aims at describing the instabilities leading to the development of bubbles in the ionospheric medium. Drawing up a model to predict electron density to the second order relies on solving the medium's fluid equations as described earlier. This second order model only takes the momentum and continuity equations into account [9]. Gravitational terms and recombination of electrons are not considered. The continuity equation can be written as:

$$\frac{\partial N_\mathrm{i}}{\partial t} + \nabla.(N_\mathrm{i} v_\mathrm{i}) = P_\mathrm{i} - L_\mathrm{i} \tag{3}$$

In what follows, we assume that the production and loss rates of electrons are set to zero. The first hypothesis corresponds to nighttime and the second to high altitudes, typically the F layer and above.

The momentum equation can be written as:

$$v_\mathrm{i} - v_\mathrm{n} = \frac{\Omega_\mathrm{i}}{\upsilon_\mathrm{i}}\left[\frac{E}{B} - v_\mathrm{i} x\hat{z}\right] + \frac{1}{\upsilon_\mathrm{i}}\left[\frac{\partial}{\partial t} + v_\mathrm{i}.\nabla\right] v_\mathrm{i} \tag{4}$$

To solve these equations, the z axis is aligned with the Earth's magnetic field. Moreover, we assume that the terms related to the gradients in the electron and ion temperatures are equal to zero. The applied forces, which correspond to the right hand

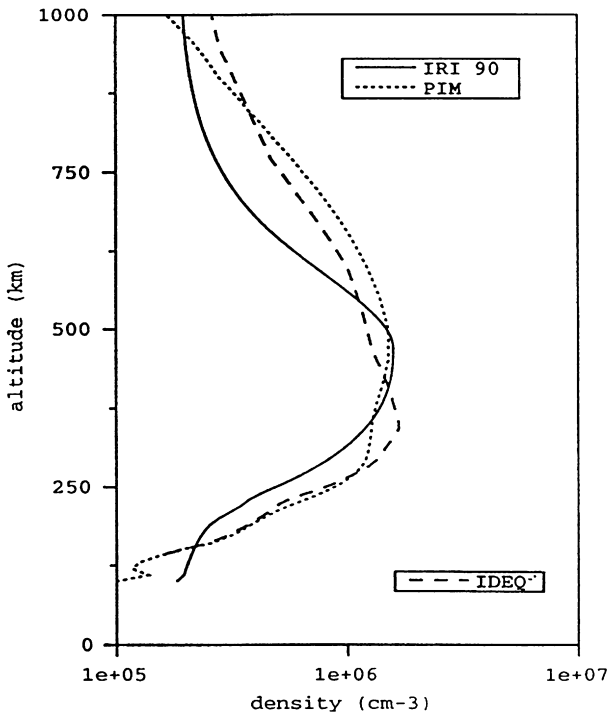

Fig. 2. Electron density vertical profile at low latitudes compared with two reference models: IRI 90 and PIM [8]. The two physical models (IDEQ and PIM) compare quite well. Major discrepancies arise above the peak. This was obtained for 12 Local time at 11.95° South and 76°87 West. The solar flux was F10.7 = 150.

side of the equation, are linked to the local electromagnetic field. The two terms used in the previous equation apply to the $E \times B$ gradient drift instability and to the Kelvin–Helmholtz instability corresponding to the magnetosphere–ionosphere coupling.

3.1. Algorithm

The above equations are transformed using the indicated hypothesis, assuming that the electric field is of electrostatic nature. Noting Φ, the electrostatic potential, the continuity equation is written as a differential equation versus time:

$$\frac{\partial N}{\partial t} = \frac{1}{B}\left[\frac{\partial \Phi}{\partial y}\frac{\partial N}{\partial x} - \frac{\partial \Phi}{\partial x}\frac{\partial N}{\partial y}\right] \tag{5}$$

The momentum equation is an elliptic equation:

$$\nabla.N\nabla\Phi = -BV_{\mathrm{n}}\frac{\partial N}{\partial y} \tag{6}$$

The local electric field is assumed to be aligned with the x axis. The medium is electrically neutral. As we ignored the coupling between different altitude layers, the terms linked to the Kelvin–Helmholtz instability have been omitted from the above equation.

The domain of analysis is rectangular. A periodical boundary condition is assigned on the y axis and a Neumann boundary condition is assigned on the x axis. The periodicity along the drift velocity (y or $E \times B$) axis allows letting the medium irregularities develop without introducing arbitrary boundary conditions. When starting the calculation, the electronic density is imposed on a strip (a few lines) in direction transverse to the $E \times B$ direction (cf. Fig. 3). The electron density impulse has a Gaussian shape as shown on this figure.

The continuity and momentum equations are successively solved at each time step. The momentum equation provides the scalar potential at every mesh point. The values obtained are then used in the continuity equation to calculate the electron density at the next time step.

In the calculations performed, the space step was set to one km on the x axis and to 250 m on the y axis. This results in solving large size problems which typically involve several thousand points for analyzed areas representing tens of km on each one of the axis. This is done using the Incomplete Cholesky Conjugate Gradient technique (ICCG).

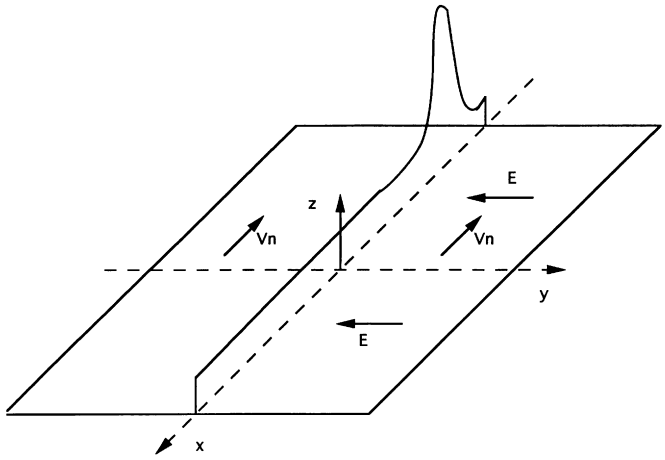

Fig. 3. Electron density impulse.

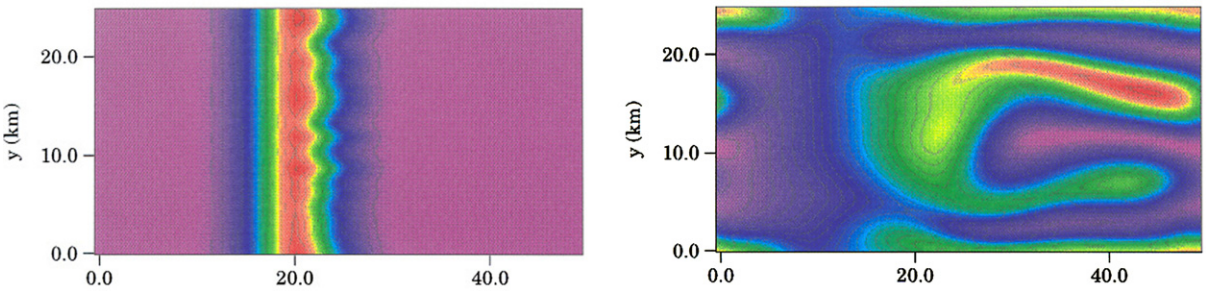

Fig. 4. Bubble development in a plane perpendicular to the magnetic field: left panel 20 s after impulse; right panel: 140 s after impulse.

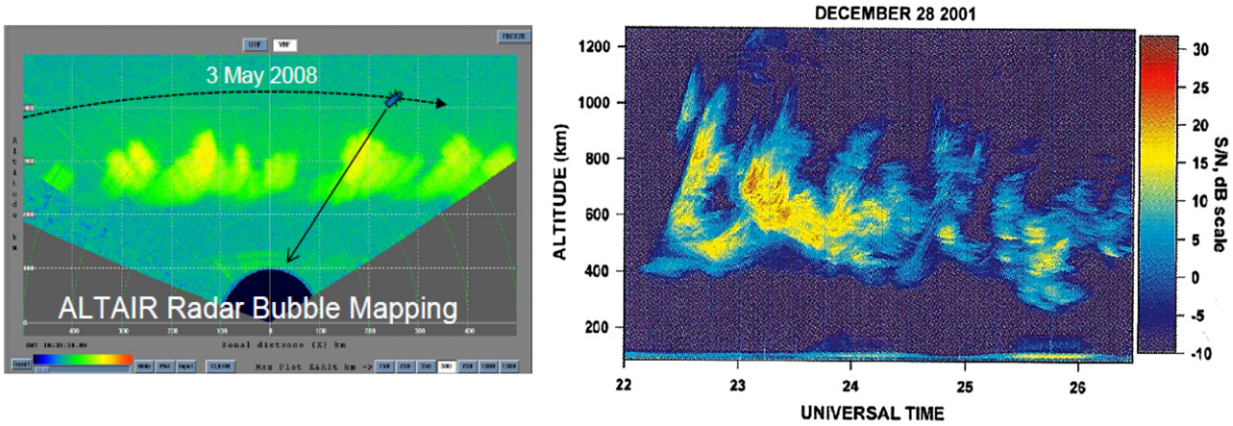

Fig. 5. Development of inhomogeneities. Radar observation at Kwajalen Islands (left panel) (courtesy K. Groves, AFRL, Boston) and in Brazil (right panel) (courtesy E. De Paula, INPE, Sao Jose dos Campos).

An example of result obtained after 140 s is presented on Fig. 4. The dimensions of the analyzed area are 25 km $\times$ 50 km. The medium appears to be striated and these striations develop along the $E \times B$ direction. Increasing the analysis time leads to a breaking of these structures into smaller ones.

Considering additional terms in the equations in order to let the coupling between different altitude layers to develop should allow obtaining the global picture of the fluctuating medium as shown on observations presented on Fig. 5 (K. Groves et al. [10] and Rodrigues et al. [11]). The vertical extent may reach values up to 100 km.

4. Conclusion

Two ionosphere models allowing the calculating of the electron density inside the medium were presented. The first model is a large scale model. It allows estimating the electron density on distances as large as several hundreds of kilometers of height and several tenths of latitude degrees on both sides of the magnetic equator. The model reproduces the F layer ionization peak and the equatorial anomaly. Although some assumptions were made in order to simplify the equations, the global behavior is accurately estimated and the relative importance of the parameters can be assessed.

The second model is a small scale model; it allows estimating the bubbles size and behavior with respect to the time. The gradient drift instability is the instability process which was considered. This second model could be improved including additional interactions involving in particular the coupling between different altitudes in order to get the plumes shapes as shown on Fig. 5. This work is currently in progress.

References

[1] Y. Béniguel, J.-P. Adam, A. Bourdillon, P. Lassudrie-Duchesne, Ionospheric scintillation effects on navigation systems, C. R. Physique 12 (2) (2011) 186–191, this issue.
[2] Don Huton, O. De la Beaujardière, C/NOFS press conference, AGU December 2008.
[3] G.J. Bailey, R. Sellek, Y. Rippeth, A modeling study of equatorial topside ionosphere, Annales Geophysicae 11 (1993) 263.
[4] G.J. Bailey, R. Sellek, A mathematical model of the earth's plasmasphere and its application in a study of He^+ at $L = 3$, Annales Geophysicae 8 (3) (1990) 171–190.
[5] C. Mc Ilwain, Coordinates for mapping the distribution of mathematically trapped particles, Journal of Geophysical Research 66 (11) (1961) 3681–3691.
[6] D. Bilitza, Solar terrestrial models and application software, Planetary and Space Science 40 (4) (1992) 541–544.
[7] R. Daniell, L. Brown, D. Anderson, M. Fox, P. Doherty, D. Decker, J. Sokja, R. Schunk, Parametrized ionospheric model: a global ionospheric parametrization based on first principle models, Radio Science 30 (5) (September–October 1995) 1499–1510.
[8] A. Preble, D. Anderson, B. Fejer, P. Doherty, Comparison between calculated and observed F region electron density profiles at Jicamarca, Peru, Radio Science 29 (4) (July–August 1994) 857–866.
[9] Y. Béniguel, Model of development of inhomogeneities inside the ionosphere, in: Symposium Proceedings on Environment Modelling for Space-Based Applications, ESTEC, Noordwijk, September 1996.
[10] K. Groves, C. Carano, Scintillation impacts on GPS, in: Workshop for Sustainable Development in Navigation Studies and Technology in Africa, Trieste, April 2009.
[11] F. Rodrigues, E.R. De Paula, M. Abdu, A. Jardim, K. Iyer, P. Kintner, D. Hysel, Equatorial spread F irregularity characteristics over Sao Luis, Brazil, using VHF radar and GPS scintillation techniques, Radio Science (2004), doi:10.1029/2002RS002826.